ELSEVIER

Journal of Magnetism and Magnetic Materials 231 (2001) 162–171

Journal of magnetism and magnetic materials

www.elsevier.com/locate/jmmm

Magnetic ordering of $PrCoAl_4$ a neutron diffraction study

P. Schobinger-Papamantellos[a,*], G. André[b], J. Rodriguez-Carvajal[b], O. Moze[c], W. Kockelmann[d,1], L.D. Tung[e,2], K.H.J. Buschow[e]

[a] *Laboratorium für Kristallographie, ETHZ CH-8092 Zürich, Switzerland*
[b] *Laboratoire Léon Brillouin (CEA-CNRS), Centre d'Etudes de Saclay, 91191, Gif-sur-Yvette, France*
[c] *INFM, Department of Physics, University of Modena and Reggio Emilia Via G. Campi 213/a, A-4110 Modena, Italy*
[d] *Mineralogical-Petrological Institute, University of Bonn, D 53115 Germany*
[e] *Van der Waals-Zeeman Institute, University of Amsterdam Valckenierstr. 65, 1018 XE Amsterdam, The Netherlands*

Received 6 July 2000

Abstract

The magnetic ordering of the orthorhombic (Pmma space group) $PrCoAl_4$ compound has been studied by neutron diffraction. Only the Pr moments order. Below $T_N = 17$ K they adopt a longitudinal amplitude modulated structure. The magnetic moments are confined to the c direction with the wave vector $\mathbf{q} = (0, 0, q_z)$ with an almost temperature independent length. At 1.5 K the amplitude of the wave is 2.24(4) μ_B/Pr atom and the wave vector $q_z = 0.437(2)$ can be approximated within error limits by a rational fraction $\frac{11}{25}$ which alternatively gives the possibility to consider the structure as a commensurate phase.

Keywords: Rare earth cobalt aluminide; Neutron diffraction; Magnetic structure

1. Introduction and magnetic properties

The $RCoAl_4$ compounds exist only for R = La, Ce and Pr. These compounds crystallise in the orthorhombic $LaCoAl_4$ type of structure (space group Pmma, $a = 7.629$ Å, $b = 4.037$ Å, $c = 6.870$ Å, $z = 2$, R: $2e(\frac{1}{4}, 0, z)$, $z = 0.382$; Co: $2e, z = 0.816$; Al1: $2a : (0\,0\,0)$; Al2: $2f : (\frac{1}{4}, \frac{1}{2}, z)$, $z = 0.043$; Al3: $4j : (x, \frac{1}{2}, z)$, $x = 0.069$, $z = 0.702$) [1].

Structural investigations on $CeCoAl_4$ [2] has shown that there is no site-disorder and the rare-earth atom is primarily surrounded by the Al atoms. The magnetic properties of a $CeCoAl_4$ single crystal reported earlier [3] indicate that: (i) the Co atoms are non-magnetic and the Ce moments order antiferromagnetically below $T_N = 13.5$ K; (ii) Ce is trivalent and the magnetic properties of this compound are entirely due to the Ce–Ce exchange interaction and the magnetocrystalline anisotropy.

The magnetic properties of a $PrCoAl_4$ single crystal [3,4] has shown that the Co atoms are non-magnetic and that the Pr moments order

*Corresponding author. Tel.: +41-1-632-3773; fax: +41-1-632-1133.
E-mail addresses: schobinger@kristall.erdw.ethz.ch, nelly@kristall.erdw.ethz.ch (P. Schobinger-Papamantellos).

[1] Now at ISIS Facility, Rutherford Appleton Laboratory, Didcot, OX11 0QX, UK.

[2] Present address: ITIMS, 1 Dai Co Viet street, Hanoi, Vietnam.

0304-8853/01/$ - see front matter
PII: S0304-8853(01)00062-2

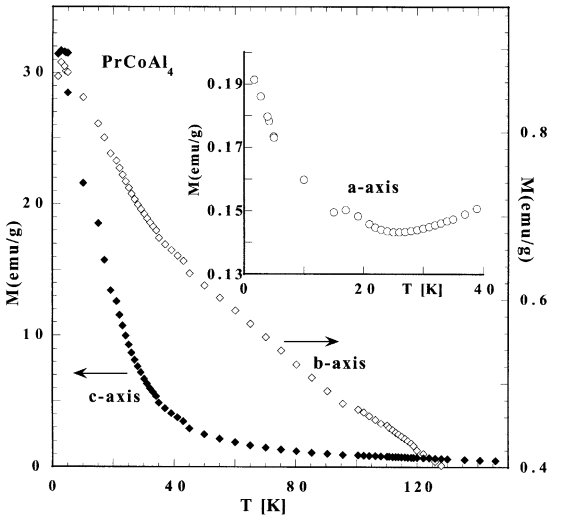

Fig. 1. Temperature dependence of the magnetization of $PrCoAl_4$, measured with a field of 1 T applied along the $a\times$ (inset) b and c directions of a single crystal.

antiferromagnetically at low temperature. In the temperature dependence of the reciprocal susceptibility measured along the a-axis, three peaks were observed at 35, 26 and 15 K (Fig. 1 in Ref. [4]). However, it is dubious whether peaks in the temperature dependence of the reciprocal susceptibility can give any indications of magnetic ordering events (see also below). The field dependence of the magnetisation at 4.2 K is strongly anisotropic [4]. Along the c-axis, the Pr moments become forced ferromagnetic after a spin-flop transition at about 0.7 T, reaching $3\,\mu_B$/Pr at highest field applied (20 T). The magnetic isotherms remain linear along the b- and a-axes, and even at 20 T the Pr moments are still far from being forced into the parallel direction. Measurements of the temperature dependence of the magnetization made on the same single crystal are shown in Fig. 1. The magnetization adopts only very small values when measured perpendicular to the c direction. The data shown in Fig. 1 were made in a field of 1 T, which is above the spin-flop field. These data suggest that magnetic ordering occurs below about 20 K.

The magnetic structure of both the $CeCoAl_4$ and $PrCoAl_4$ compounds have not been studied before. Preliminary neutron diffraction tests of a $PrCoAl_4$ single crystal [5] in the temperature range 11–40 K using the LADI Laue-Diffractometer at the ILL, Grenoble, indicated that long range magnetic order only sets in at about 16 K and is associated with the wave vector $\mathbf{q} = (0, 0, 0.405)$ r.l.u. These results are in agreement with the results of the magnetic measurements. Neutron data were also taken on a powder sample of $PrCoAl_4$ for a few temperatures at the ISIS facility [6]. These data indicated that magnetic satellites occur at positions different from nuclear reflections or corresponding to simple cell multiples. Furthermore, the powder sample was found to contain small amounts of an impurity phase.

The present study reports on the magnetic structure of $PrCoAl_4$ on the basis of powder neutron data, including neutron time-of-flight (TOF) data, using the same sample as in [6].

2. Neutron diffraction

2.1. Data collection and analysis

Neutron diffraction experiments were carried out in the temperature range 1.5–46 K at two different facilities: (a) Data were collected at the Orphée reactor (LLB-Saclay) on the G4.1 (800-cell Position Sensitive Detector: PSD) diffractometer using the wavelength of 2.426 Å. The data were collected for a full set of temperatures in the range 1.5–46 K in steps of 3 K in order to study more precisely the magnetic transitions. The step increment in 2θ was 0.1° and the 2θ region $8–87^\circ$ (b) At the ISIS spallation neutron source, Didcot, UK on the ROTAX time-of-flight neutron powder diffractometer [7] in the paramagnetic state at 65 K and in the magnetically ordered state at 15 K. The data were collected simultaneously in two separate detector banks, located at scattering angles of $2\theta = 28.12^\circ$ and 125.5°. The TOF paramagnetic data were used for structural refinements. All data sets were analysed with the program FullProf [8].

2.2. Crystal structure

The refinement of the diffraction pattern collected in the paramagnetic state at 45.7 K (G41

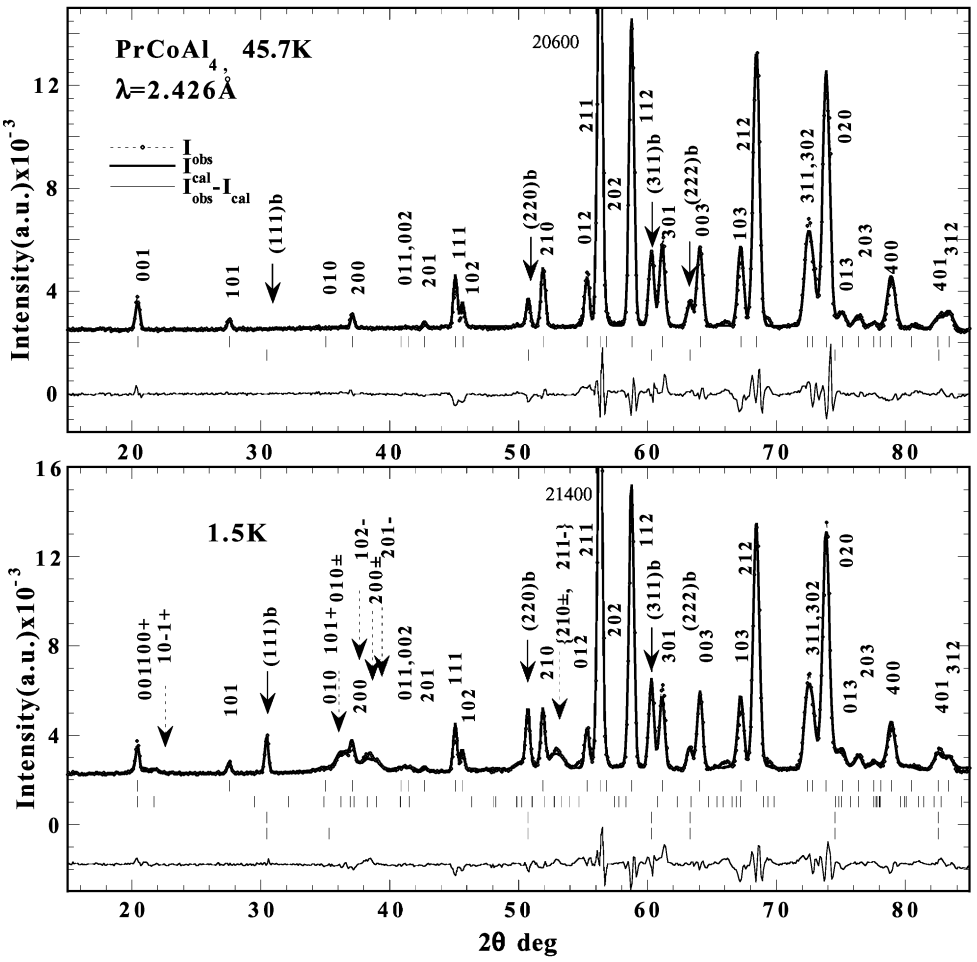

Fig. 2. Observed and calculated neutron intensities of $PrCoAl_4$, in the paramagnetic state at 45.7 K (top part) and the magnetically ordered state at 1.5 K (bottom part).

data) and 65 K (TOF data) have shown that the sample contains a small amount (about 6%) of $PrAl_2$ as an impurity phase which partly does not overlap with the reflections of the main phase $PrCoAl_4$. The $PrAl_2$ reflections are indexed as $(h\,k\,l)b$ and are denoted by full arrows in the top part of Fig. 2. This phase was included in the refinement (Fd3m space group, $MgCu_2$ structure-type $a = 8.028(2)$ Å). Results of the two refinements are summarised in Table 1 and Figs. 2 and 3 confirm the $PrCoAl_4$ structure [1]. In this structure the Pr atoms form double layers ($MgCuAl_2$-type slabs) perpendicular to the c direction. As can be seen in Fig. 4, these are separated by the slabs of the Al polyhedra. The Co atoms are located in the centres of the trigonal prisms formed by Al2 and Al3 atoms.

2.3. Magnetic ordering

The neutron patterns collected below 34 K contain additional reflections of magnetic origin at positions different from those of the nuclear reflections. The first set consists of only a few well resolved magnetic reflections (denoted by $(1\,1\,1)b$ and $(2\,2\,0)b$ in Fig. 2, bottom part). These

Table 1
Refined structural parameters of $PrCoAl_4$ from neutron data in the paramagnetic state at 45.7 K (G41 data) and 65 K(TOF data) and the magnetically ordered state at 1.5 K (Pmma Space Group)[a]

Pmma	65 K	TOF		45.7 K	G41	1.5 K		
Atom/site	x	z	B_i (Å)^2	x	Z	x	z	μ_{oz} (μ_B)
Pr: 2*e*	0.25	0.3840_3	0.324_3	0.25	0.3853_9	0.25	0.386_1	2.24_4
Co: 2*e*	0.25	0.8128_6	0.305_5	0.25	0.8086_2	0.25	0.807_1	
Al1: 2*a*	0.0	0	0.51_4	0.0	0	0	0	
Al2: 2*f*	0.25	0.0437_4	0.41_4	0.25	0.039_1	0.25	0.037_1	
Al3: 4*j*	0.0694_2	0.6997_3	0.26_3	0.0677_7	0.7012_8	0.069_1	0.696_1	
a (Å)	7.6351_1			7.647_1		7.644_1		
b (Å)	4.040637			4.0438_5		4.0431_4		
c (Å)	6.8688_1			6.874_1		6.8717_8		
R_n	5.26			6		4.6		
R_m (%)	—			—		13.4		
R_{wp} (%)	11.1			13.5, 3.0		13.8		
R_{exp} (%)	4.8					3.0		

[a] Pr and Co occupy the 2*e* : ($\frac{1}{4}$, 0, *z*) positions and Al three sites Al1: 2*a*(0 0 0); Al2: 2*f*($\frac{1}{4}$, $\frac{1}{2}$, *z*) and Al3: 4*j*(*x*, $\frac{1}{2}$, *z*). B_i is the individual temperature factor was set to the same value for the G41 data. $R_n, R_m, R_{wp}, R_{exp}$ are the residuals for the integrated nuclear and magnetic, the weighted profile and the experimental intensities. $\mu_{oz}(\mu_B)$, is the refined amplitude of the Pr^{3+} sine wave along the *c*-axis with the wave vector $\mathbf{q} = (0, 0, 0.437(2))$ r.l.u.

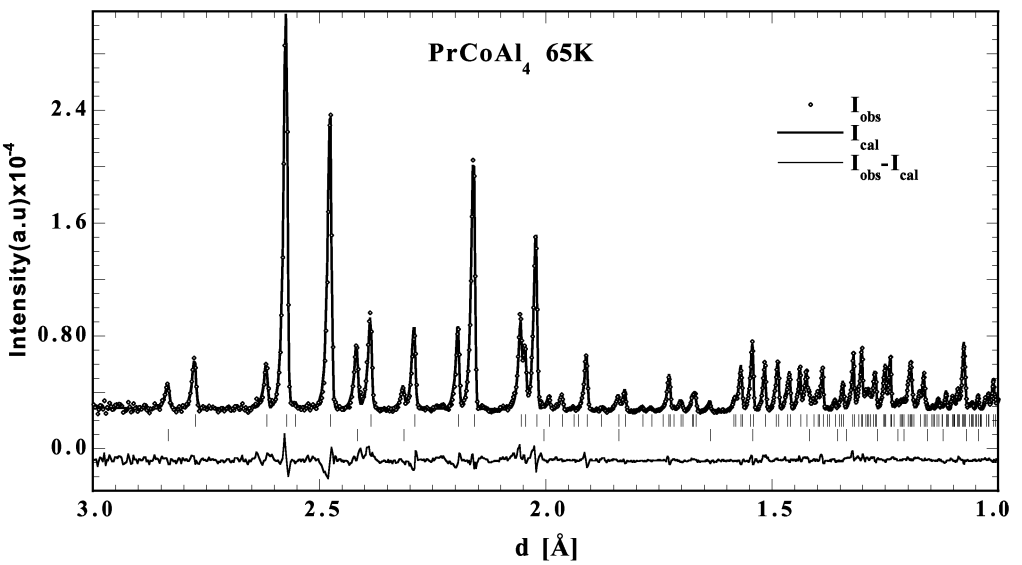

Fig. 3. Intensity versus *d*-spacing (Å) (neutron time-of-flight data) of $PrCoAl_4$ in the paramagnetic state at 65 K, collected in the backscattering detector bank, located at $2\theta = 125.5^\circ$. Reflections markers at the top refer to the main $PrCoAl_4$ phase, whilst those at the bottom refer to the impurity $PrAl_2$ phase.

reflections appear below 34 K at 2θ positions of 30.5° and 50.5°, respectively. They pertain to the $PrAl_2$ ferromagnetic ordering with $T_C = 34$ K and were included in the refinement.

Below 20 K a second set of not well resolved, weak and broad magnetic contributions evolved around the nuclear reflection (2 0 0) at $2\theta = 37^\circ$ and on the right side of reflection (2 1 0). The latter

observation suggested a wave vector direction along the c-axis. Several combinations of wave vectors were used in profile matching trials and it has been possible to index all magnetic satellites with a single wave vector along the c direction with $q_z = 0.437(2)$ r.l.u. Fig. 5 displays in more detail the distribution of the group of magnetic reflections around the (2 0 0) position. The different width of the magnetic reflections could be approximated using a domain size Gauss parameter in the refinement [9] that led to an average domain size of 177Å for the magnetic reflections.

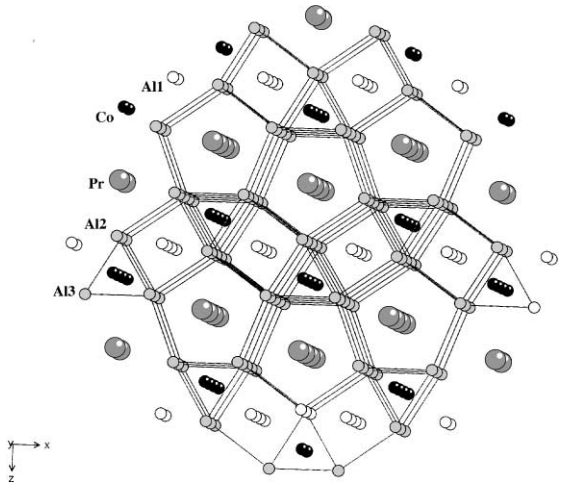

Fig. 4. Three-dimensional schematic representation of the $PrCoAl_4$ structure indicating the double layered character of Pr perpendicular to the c-axis separated by the slabs of Al polyhedra.

The absence of $0\,0\,\ell \pm \mathbf{q}$ satellites including the $0\,0\,0 \pm \mathbf{q}$ satellite suggests either an antiparallel arrangement of the magnetic atoms within the elementary cell or a moment direction along the c-axis, and in a first approximation, a longitudinal amplitude modulated magnetic structure. Symmetry analysis suggests that the two Pr atoms related by the centre of symmetry belong to two distinct orbits. This means they could have different moment values and different orientations. However, the refinement has converged with a parallel arrangement of the two Pr moments within the chemical cell (see Fig. 6a) and has confirmed the longitudinal amplitude modulated structure. In such a structure the moment component of the Pr atoms in the nth cell is given by the expression:

$$\boldsymbol{\mu}_{nj} = \mu_{0j}\mathbf{z}\cos(2\pi\mathbf{q}\cdot\mathbf{R}_n + \phi_j), \tag{1}$$

where $\mathbf{z}$ is a unit vector in the direction of the varying moment component, μ_{0j} the amplitude of the sinusoidal variation. The quantity ϕ_j represents a phase factor of the jth atom relative to the origin of the wave usually taken at atom (1) and with $\mathbf{R}_n = n_1 a + n_2 b + n_3 c$, in the nth cell (n is integer and $j = 1$). In our case the phase between the two Pr atoms was $\phi = 0$

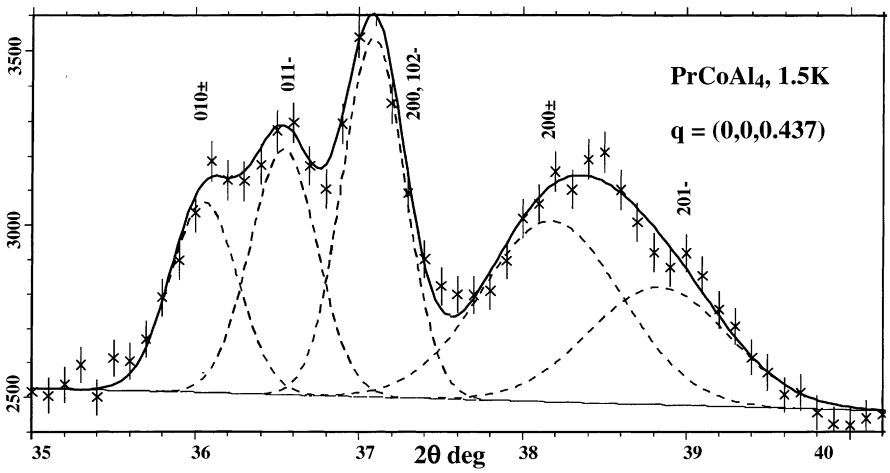

Fig. 5. Magnetic satellite distribution around the 200 nuclear reflection.

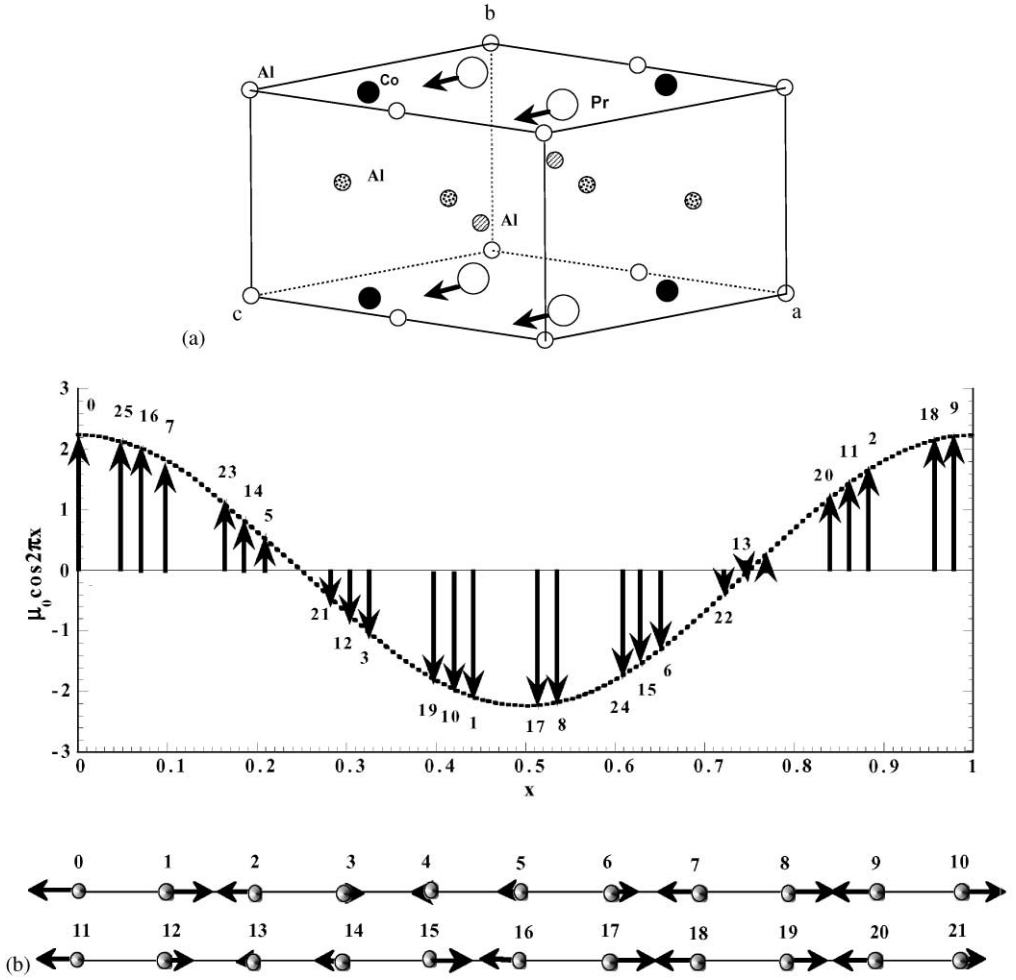

Fig. 6. (a) The Pr magnetic moment arrangement within the zeroth cell in $PrCoAl_4$. The magnetic moment length changes collectively from cell to cell in the direction of the wave vector. (b) The calculated $\mu_z \| c$, Pr moment component for $n = 25 \times c$ cells as for the obseved longitudinal sine wave modulation ($\mu_0 \cos 2,\ x = qn + \varphi$) with the wave vector $q = (0, 0, 0.442(2))$ at 1.5 K. The refined amplitude value is $\mu_0 = 2.24\,\mu_B$ and $\varphi = 0$. Also shown is the moment distribution in 20 successive cells (in two rows) along the c-axis.

Within the error limits the wave vector $q_z = 0.437(2)$ r.l.u. can be approximated by a rational fraction having the value $0.44 = \frac{11}{25}$. This means that the structure can alternatively be considered as a commensurate structure in a $25 \times c$ larger cell. In Fig. 6b the Pr moment components along c are calculated for $25 \times c$ cells for $q_z = 0.442$ r.l.u. and the phase $\phi = 0$ that is why the 25th atom has a smaller moment value of that on the zeroth cell. The real structure is shown in the bottom part of the same figure for only 20 cells along c (in two rows). The refined amplitude of the wave at 1.5 K equals $2.24\,\mu_B$, which is inferior to the Pr^{3+} free ion moment value $g\mathbf{J}\mu_B = 3.2\,\mu_B$. This is most likely due to the presence of crystalline field effects. Another reason for the reduced moment value may be sought in the presence of disorder usually found in magnetic modulated structures and/or in the presence of co-existing short-range order effects (Table 2).

Table 2
Observed and calculated nuclear and magnetic integrated neutron intensities of $PrCoAl_4$ at 1.4 K ($\lambda = 2.426$ Å) with the magnetic wave vector $\mathbf{q} = (0, 0, 0.437(2))$

h	k	l	$\pm\mathbf{q}$	$2\theta^\circ$	I_{calc}	I_{obs}
1	0	0	±	20.305	152	197
0	0	1		20.338	401	475
1	0	1	+	21.616	264	264
1	0	1		27.466	196	170
1	0	−1	−	34.777	135	122
0	1	0		34.914	2	1
0	1	0	±	36.074	706	666
0	1	1	−	36.864	590	565
2	0	0		37.013	218	197
1	0	−2	−	37.174	113	113
2	0	0	±	38.118	545	545
2	0	−1	−	38.872	437	571
1	1	0	±	40.722	115	100
0	1	1		40.740	3	3
0	0	2		41.354	0	0
1	1	1	+	41.437	176	146
2	0	1		42.595	73	61
1	1	1		44.984	788	643
1	0	2		45.552	371	279
0	1	1	+	46.230	58	30
2	0	1	−	47.914	45	30
0	1	−2	+	48.149	33	20
2	0	−2	−	49.784	26	27
1	−1	1	+	50.104	348	342
2	1	0		51.793	966	960
1	1	−2	+	51.916	329	334
2	1	0	±	52.645	546	585
2	1	1	−	53.233	483	525
1	0	2	+	54.535	28	66
0	1	2		55.204	804	971
2	1	1		56.209	8832	9222
2	0	2		56.692	120	106
1	0	3	−	57.367	21	25
3	0	0	±	57.666	22	25
3	0	1	−	58.219	34	37
1	1	2		58.649	6251	6032
2	1	1	−	60.642	78	92
3	0	1		61.035	1678	2057
2	1	2	−	62.245	47	57
0	1	2	−	63.218	4	6
0	0	3		63.964	1944	1947
2	0	2	−	64.591	4	3
3	0	1	−	65.268	102	156
0	1	−3	+	65.818	6	12
1	1	−2	+	66.469	132	171
3	0	−2	+	66.81	102	97
2	0	3	+	67.162	6	5
2	1	2		68.337	6697	6791
1	−1	3	−	68.945	107	134
3	1	0	±	69.214	33	45
3	1	1	−	69.715	53	73
3	1	1		72.284	1947	2190

Table 2 (*continued*)

h	k	l	$\pm\mathbf{q}$	$2\theta^\circ$	I_{calc}	I_{obs}
3	0	2		72.707	1610	1619
0	2	0		73.593	2267	2442
0	2	0	±	74.437	90	94
0	2	1	−	74.925	129	125
0	1	3		74.992	497	453
2	−1	2	−	75.576	8	8
2	0	3		76.265	389	411
3	1	1	−	76.209	173	181
0	2	1		77.425	109	123
1	2	0	±	77.413	35	36
1	0	3	+	77.622	2	2
3	−1	−2	+	77.654	178	175
1	2	1	+	77.893	56	51
2	−1	3	+	77.987	14	12
1	1	3		77.961	68	55
4	0	0		78.814	1655	1476
4	0	0	±	79.500	102	105
3	0	−2	−	79.793	59	67
4	0	1	+	79.977	93	112
1	0	−4	−	80.966	1	2
1	2	1		80.367	82	112
0	2	1	+	81.268	30	53
3	0	3	−	82.169	50	60
4	0	1		82.435	385	436
0	2	2	−	82.690	19	20
3	1	2		83.265	519	499
1	−2	−1	−	84.178	186	80
0	1	−3	+	85.138	15	10
2	2	0		85.495	157	139
1	2	−2	+	85.592	190	161
2	−2	0	±	86.170	234	215
4	0	1	+	86.231	19	18

2.4. Thermal evolution of magnetic ordering

The temperature variation of the integrated intensity of several magnetic satellites shown in Fig. 7 (top part) indicates that long-range ordering of the Pr moments sets in below 20 K. The intensities of the most dominant satellites are seen to increase smoothly with decreasing temperature. Also the thermal evolution of the amplitude of the wave shows a smooth evolution (Fig. 7, bottom part). The wave vector value seems to (within the error limits) be unchanged with temperature. Here we would like to mention that the higher the temperature the less precise are the refined parameters due to the signal weakness and the increasing magnetic peak halfwidth. For completeness we include the thermal behaviour of the (1 1 1)b and (2 2 0)b magnetic reflections of the $PrAl_2$ impurity phase (Fig. 8). This confirms the ordering temperature of 34 K reported for $PrAl_2$.

3. Discussion

The refined amplitude modulated structure can be described in simple terms as consisting of ferromagnetic Pr layers perpendicular to the (0 0 1) direction. This arrangement corresponds to ferromagnetic first neighbour interactions for distances below 4 Å. These comprise the distances along the

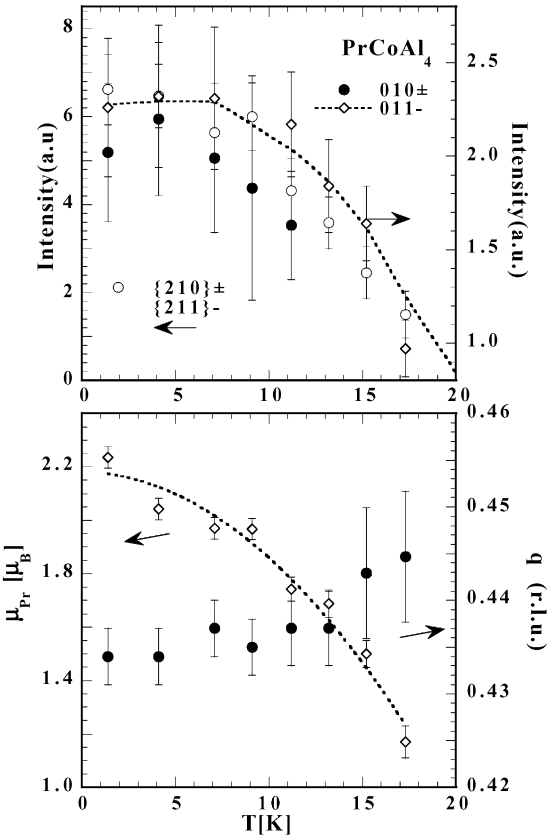

Fig. 7. Thermal variation of the intensity of several magnetic satellite reflections: $(0\,1\,0) \pm \mathbf{q}$, $(0\,1\,1) - \mathbf{q}$ and $(\{2\,1\,0\} \pm \mathbf{q}$, $\{2\,1\,1\} - \mathbf{q})$ indicating the onset of magnetic order at $T_N \leqslant 20$ K of the $PrCoAl_4$ compound (top part). Also shown is the thermal variation of the amplitude and the wave vector value.

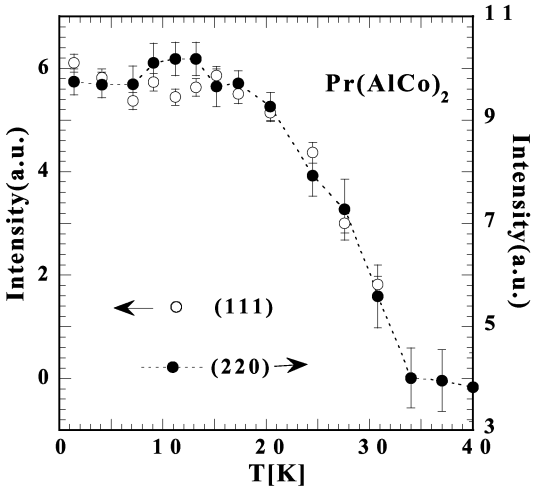

Fig. 8. Temperature dependence of the magnetic reflections $(1\,1\,1)b$ and $(2\,2\,0)$ at $2\theta = 30.5°$ and $50.5°$, respectively, pertaining to the $PrAl_2$ coexisting phase (see Fig. 2).

b axis and the shortest distance within the Pr zigzag chains along a (see also Fig. 3). The exchange interactions along the c direction correspond to longer distances ($c = 6.8$ Å) and may comprise competing interactions, as usual in incommensurate systems between first and second neighbours.

Amplitude modulated structures are widely observed in rare earth intermetallics in the high temperature region below T_N. Their existence may be related to a competition of the long-range oscillatory exchange interaction between the localised 4f moments, the crystalline electric field induced anisotropy and small quadrupole–quadrupole interactions [9,10]. The exchange interactions in rare earth intermetallic compounds are indirect and of the RKKY type, mediated by the polarisation of the conduction electrons, the radial extent of the rare earth 4f electrons being too small for direct interactions. Due to the low symmetry of rare earth site it is likely that crystal field effects become of importance and may introduce an important anisotropy and strongly fix the moment direction.

In compounds where the rare earth ions have an odd number of unpaired electrons the amplitude modulated structures become unstable at $T = 0$ K if the anisotropy is of the Ising type. In such cases a squaring up of the structure is observed and new harmonics of the main propagation vector appear. Simultaneously a trend towards a long period commensurate structure (rational components of the wave vector) is observed [10]. If the anisotropy is of the Heisenberg type the moments can still have a sinusoidal structure at 0 K, but the interpretation is not that the moment of different sites is changing in amplitude. The sinusoidal picture stands only for the long-range ordered components of the magnetic moment, the other component remaining in a disordered state. This disorder then has its origins in frustration effects.

According to theory [11] long period structures with a wave vector expressed by a rational fraction p/N, where N is odd may display odd and even harmonics. The possible evolution of ferromagnetism in such structures [12] is due to the fact that the number of + and − moments do not match. In the case of Pr^{3+} (having an even number of unpaired electrons) the ground state may be non-magnetic if the lowest crystalline electric field level is a singlet; so the observed sinusoidal structure may be stable up to 0 K.

This may explain why no higher harmonics were observed at the lowest temperatures in the powder patterns. A similar behaviour has been reported for the tetragonal $PrNi_2Si_2$ compound [13,14] that also does not display a magnetic transition at low temperatures. An analysis of the crystalline electric field interaction for the orthorhombic $PrCoAl_4$ compound would be most helpful for the understanding of the present neutron data. Such an analysis appears to be rather difficult because of the low symmetry of the structure, requiring many crystal field parameters and additional information such as results from inelastic neutron scattering and specific heat measurements.

References

[1] R.M. Rykhal, O.S. Zarechnyuk, Ya.P. Yarmolyuk, Dopov. Akad. Nauk. Ukr. RSR. Ser. A 39 (1977) 265.
[2] O. Moze, L.D. Tung, J.J.M. Franse, K.H.J. Buschow, J. Alloys Comp. 256 (1997) 45.
[3] L.D. Tung, Ph.D. Thesis, University of Amsterdam, 1998.
[4] L.D. Tung, K.H.J. Buschow. J. Alloys Compounds 291 (1999) 37.
[5] C. Wilkinson, private communication.
[6] O. Moze, W. Kockelmann, ISIS Annual Report. August 1999, experiment number RB10125.
[7] W. Kockelmann, M. Weiβer, H. Heinen, A. Kirfel, W. Schäfer, Mater. Sci. Forum 321–324 (2000) 332.
[8] J. Rodríguez-Carvajal, Physica B 192 (1993) 55. The manual of FullProf can be obtained from http://www-llb.cea.fr/fullweb/powder.htm.
[9] R.J. Elliott, Phys. Rev. 124 (2) (1961) 346.
[10] W. Selke, Phys. Rep. 170 (4) (1988) 213.
[11] D. Gignoux, D. Schmitt, Phys. Rev. B 48 17 (1993) 12682.
[12] A.R. Ball, D. Gignoux, D. Schmitt, J. Magn. Magn. Mater. 119 (1993) 96.
[13] J.A. Blanco, D. Gignoux, J.C. Gómez Sal, D. Schmitt, J. Magn. Magn. Mater. 104–107 (1992) 1273.
[14] J.A. Blanco, D. Schmitt, J.C. Gómez Sal, J. Magn. Magn. Mater. 116 (1992) 128.